Particle Accelerators
1981 Vol.11 pp.239–244
0031-2460/81/1104/0239$06.50/0

CHARACTERISTICS OF THE ETA GUN*

ARTHUR C. PAUL

Lawrence Berkeley Laboratory, University of California, Berkeley, California 94720 USA

and

V. K. NEIL, G. D. CRAIG, and T. J. FESSENDEN

Lawrence Livermore National Laboratory, University of California, Livermore, California 94550 USA

(Received June 9, 1980; in final form Feb. 11, 1981)

The Experimental Test Accelerator (ETA) is a linear induction device consisting of a 2.5-MV electron gun and ten 0.25-MV accelerating units designed to produce a 10-kA beam of electrons at 5 MeV. Calculations with the computer code EBQ as well as experimental measurements indicate that the current produced by the gun is limited by two phenomena. The first arises from the variation of particle energy with time during the pulse. Only particles with energy within a limited range can be transported by the focusing coils in the gun; therefore the variation of the gun's output current with time is determined by the coil settings. The second effect results from a collective interaction at sufficiently large current to cause a virtual cathode to form a few centimeters past the extraction grid. Operation in this regime results in greatly increased beam emittance and poor beam transport through the accelerator. Results of the code calculations are compared with experimental data and found to be in good agreement.

I. INTRODUCTION

The injector for the Experimental Test Accelerator (ETA) is a 2.5-MV, linear-induction electron gun designed to produce 10 kA of beam current. In this paper we describe the theoretical prediction of the ETA gun's characteristics, and compare these predictions with experimental data. The beam dynamics in the ETA gun were determined by calculations using the computer code EBQ.[1] This is a steady-state, azimuthally symmetric, self-consistent code. The code was used in the design of the gun to determine the equilibrium flow of electrons from the cathode, through the extraction grid, across the grid-anode region and into the hollow anode. The geometric model of the gun that is used in these calculations is shown in Fig. 1. The washer shown is an electrode with potential equal to one-half the anode voltage. Focusing solenoids are placed outside the anode, and a "bucking" coil (not shown) is located back of the cathode to reduce the axial magnetic field on the cathode surface to a minimum. Particle trajectories in the gun design were followed a distance of about 2 m from the cathode, but for this paper the trajectories were followed for only 60 cm from the cathode. The finite grid structure is not considered.

During actual operation of the gun, both the grid voltage, V_g, and the anode voltage, V_a, vary in time over a period of about 50 ns. The variation of V_a with time approximates one-half of a sine wave, so the steady-state conditions simulated with the code are never achieved. In order to gain some insight into the behavior of electrons as V_g and V_s are varied, we make separate calculations with the code for various values of V_g and V_a, thus generating characteristic curves of the gun.

II. SIMULATION OF IDEAL OPERATION

In all calculations the current, I, drawn from the cathode by the extraction grid follows the Child-Langmuir law. For a cathode of area A,

$$I = 2.3 \times 10^{-6} A V_g^{3/2}/d^2. \quad (1)$$

* Lawrence Livermore National Laboratory is operated by the University of California for the Department of Energy under Contract No. W-7405-Eng-48.

This work was performed by LLNL for the Department of Defense under DARPA (DOD) ARPA Order 3718, Amendment No. 12, monitored by NSWC under Contract No. N60921-80-PO-W0188.

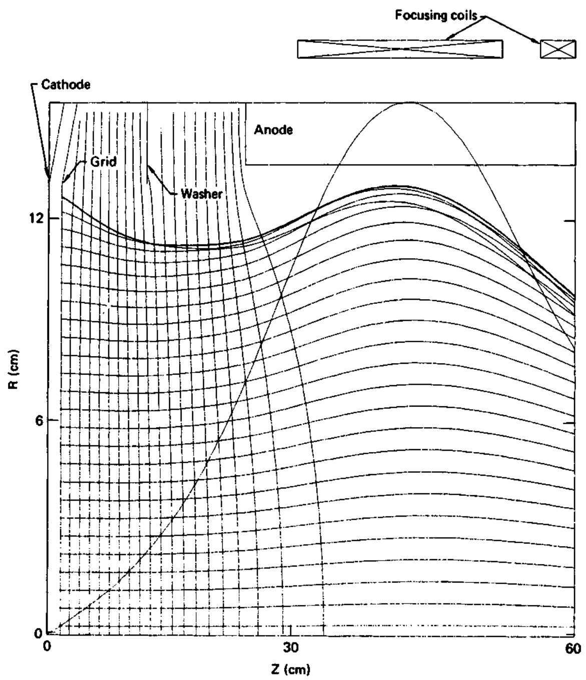

FIGURE 1 Geometry of the ETA gun, equipotential surfaces, and particle trajectories for anode voltage V_a = 2 MV, grid voltage V_g = 10 kV, and current I = 537 A.

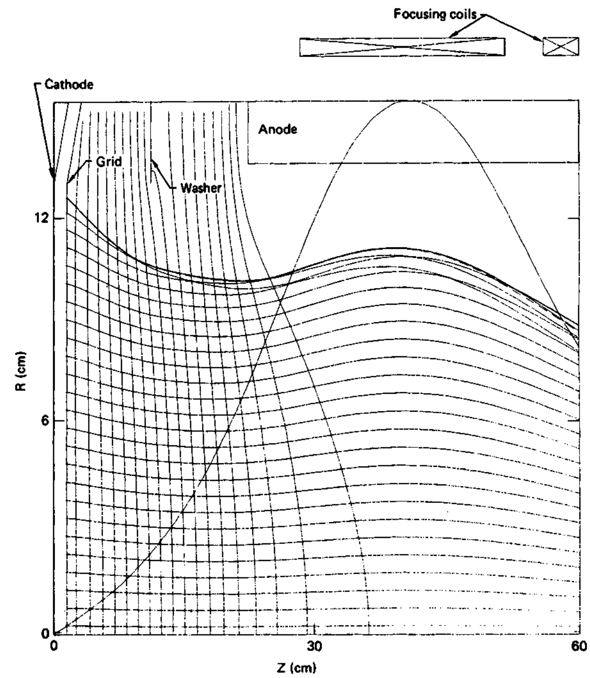

FIGURE 2 Equipotential surfaces and particle trajectories for V_a = 2 MV, V_g = 40 kV, and I = 4.27 kA.

In this relation V_g is the grid voltage in volts and d is the cathode-grid separation taken to be 1.5 cm in all calculations.

In ideal operation of the gun, the anode voltage is constant in time while the beam current is turned on by applying voltage to the grid. As the grid voltage increases the beam current increases from zero to the desired maximum value. In practice, testing has shown that the anode voltage rises too slowly to achieve this mode of operation with the present gun configuration. Ideal operation is simulated by making separate calculations with the same value of V_a and different values of V_g. Particle trajectories from a 10-inch-diameter cathode are displayed in Figs. 1, 2, and 3 for V_a = 2 MV. In these figures the approximately vertical curves are equipotentials and the approximately horizontal curves are particle trajectories. For computational convenience a Neumann boundary condition is imposed at z = 60 cm. This artificial condition does not affect results in the region of interest ($z \lesssim 40$ cm).

The bell-shaped curve is the axial magnetic focusing field at r = 0. In Fig. 1 we have V_g = 10 kV, and I = 537 A; in Fig. 2 we have V_g = 40

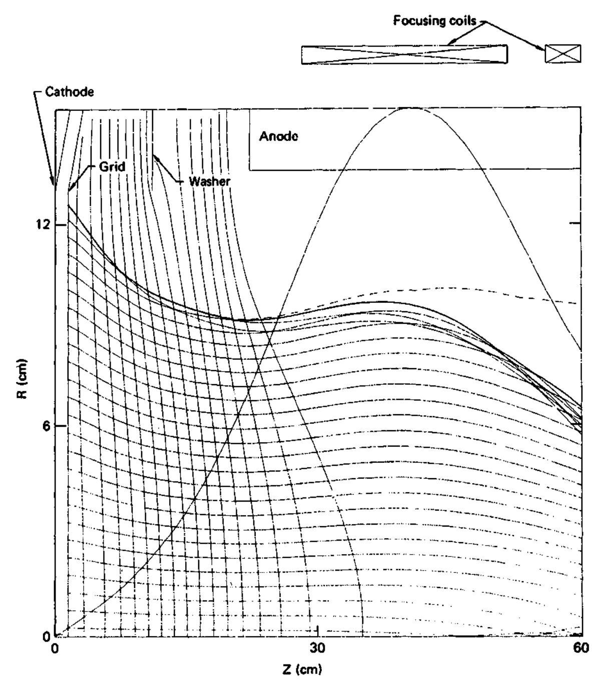

FIGURE 3 Equipotential surfaces and particle trajectories for V_a = 2 MV, V_g = 60 kV, and I = 7.82 kA.

kV and I = 4.27 kA; and in Fig. 3 we have V_g = 60 kV and I = 7.82 kA. In these three calculations the focusing solenoids are set to provide a maximum axial magnetic field B_z = 520 G on axis at a point about 40 cm from the cathode as shown in Fig. 1. The trajectories display the focusing from the azimuthal magnetic self-field in the grid-anode region. This focusing force increases with the total current.

III. WAVEFORM LIMITED TRANSPORT

The code calculations indicate that under certain circumstances current can be accelerated in the grod-anode region, but not be transported past the peak of the axial magnetic field. This occurs at low anode voltage when particles do not have enough energy to traverse the region of $B_z \approx 500$ gauss. This peak value of B_z is set to transport particles with higher energy, and the low energy particles are over-focused. The beam collapses radially and the code results become unreliable because particles are removed from the calculation when their axial velocity becomes negative. Figure 4 shows the calculated beam envelope for various anode voltages. The maximum B_z on axis is 520 gauss, and the beam-current values are chosen just below the limiting current for virtual cathode formation. At $V_a \leq 1$ MV the beam collapses downstream from the peak magnetic field, while for $V_a \geq 1.5$ MV all of the current is transported.

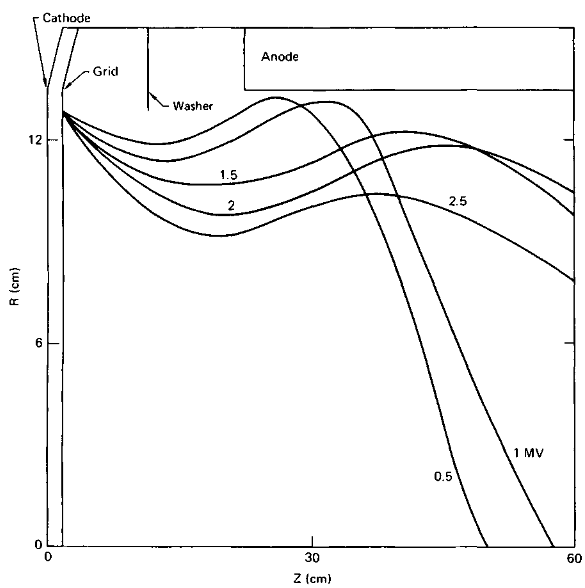

FIGURE 4 Beam envelopes for various values of anode voltage. In these calculations the value of the current is slightly below the limiting current for virtual cathode formation.

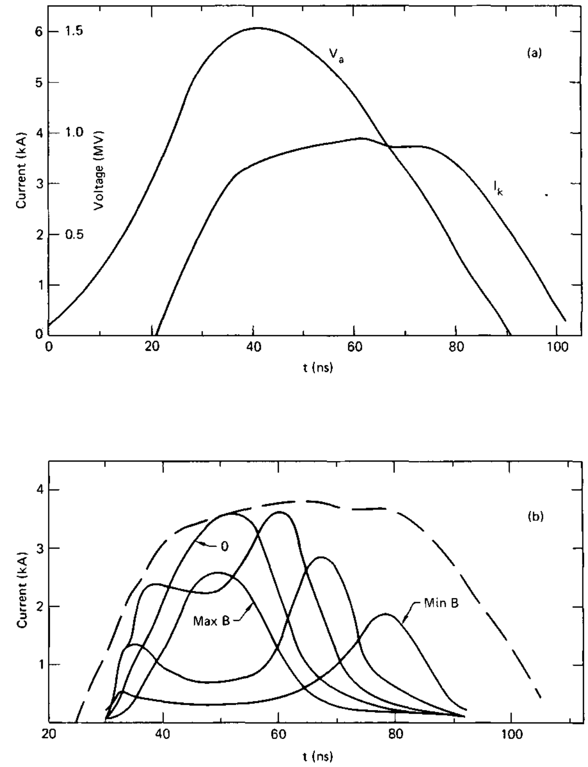

FIGURE 5 Oscillograms of voltage and beam current: (a) anode voltage and cathode current vs time; (b) beam current vs time at the gun output for five values of the peak axial magnetic field. The dashed curve is the cathode current.

This phenomenon can easily be seen in experiments by changing the strength of only the first gun focus coil and observing the current pulse at the gun output. Figure 5 shows experimental results obtained on December 5, 1979, when a 10-inch-diameter cathode was used. As shown in Fig. 5(a) the system timing was such that the current pulse emitted from the cathode was delayed by approximately 20 ns with respect to the anode voltage pulse. As a result, particles in the leading edge of the current pulse had more energy than those in the trailing edge. Figure 5(b) shows oscillograms of the gun output current as the current in the gun focus coil was varied. Transmission of the low energy particles in the trailing edge of the current pulse is improved by lowering the current in the coil, while transmission of the relatively high energy particles in the leading edge and central portion of the current pulse is degraded. The dotted envelope of these oscillograms is the current pulse emitted from the cathode, and it represents the maximum current that could be expected at the gun output. Our usual procedure is to "tune" the transport for maximum peak current. This procedure results in the selection of a waveform such as that labeled "0."

These oscillograms also illustrate two other phenomena that deserve comment. First, the pulse width of the beam current injected into the accelerator is determined by the relative timing of the cathode current and anode voltage as well as by the waveforms of these pulses. In general this timing depends on many factors in the operation of the system, and as a result the timing adjustment is difficult to optimize. Second, as the field produced by the first focus coil is adjusted higher than optimum, the pulse width narrows further and the peak amplitude decreases.

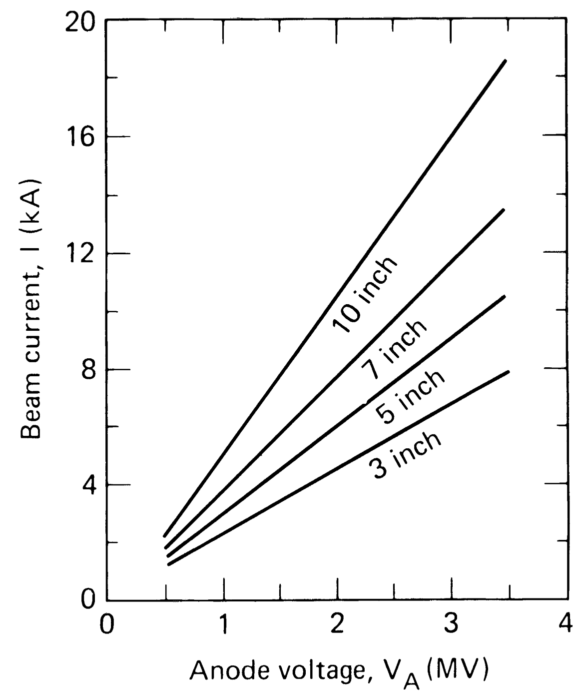

FIGURE 6 Limiting beam current for virtual cathode formation vs anode voltage for 4 cathode diameters.

IV. VIRTUAL CATHODE FORMATION

The formation of a virtual cathode limits the maximum current that can be accelerated by the gun. The current drawn from the cathode by the grid enters the grid-anode region and is accelerated if the anode voltage is sufficiently high. If the anode voltage is not sufficiently high, the results of the calculations show that a virtual cathode forms near the axis a few cm downstream from the grid. The code is not capable of calculations beyond this point. The calculated limiting current that can be accelerated is very nearly a linear function of V_a. It is shown to be linear in the artist's rendition in Fig. 6 for various diameter cathodes, but the actual theoretical curves drop slightly below the lines at higher values of V_a, as shown in Fig. 7 for a 10-inch-diameter cathode. All experimental results discussed in this section were obtained with a 10-inch-diameter cathode.

For each value of the limiting current shown in Fig. 6 there is a corresponding value of V_g found from Eq. (1). In Fig. 8 the value of V_g required to extract the limiting current is plotted vs V_a. Values of V_g above a given curve result in virtual cathode formation. Calculations indicate that the value of V_g is critical, and a variation of 1 kV in V_g is sufficient to cross from a region

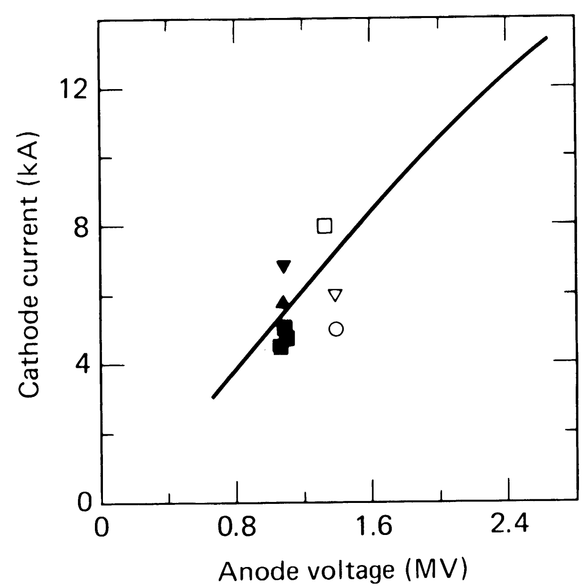

FIGURE 7 Limiting beam current for virtual cathode formation vs anode voltage for a 10-inch-diameter cathode and data points indicating eight separate experiments.

of good beam production (below the curve) to virtual cathode formation (above the curve).

It is not surprising that the maximum current that can be accelerated does not obey the relativistic Child-Langmuir law for a one-dimensional diode in the grid-anode region.[2] The grid-anode spacing is less than the diameter of the anode. The equipotential surfaces are complicated and change significantly as the current changes, so that the configuration of accelerating electric field bears scant resemblance to a planar diode.

Experiments with a 10-inch-diameter cathode show that there is a definite difference between the beam behavior operating above and that operating below the limiting grid voltage. The code cannot be used in the calculations once a virtual cathode is formed. In the experiment, current is indeed accelerated, and some of it is transported to the end of the gun (about 2.5 m from the cathode). However, the transported current decreases drastically in the full 10 m of the ETA accelerator. When operating below the limiting grid voltage, the fraction of the cathode current

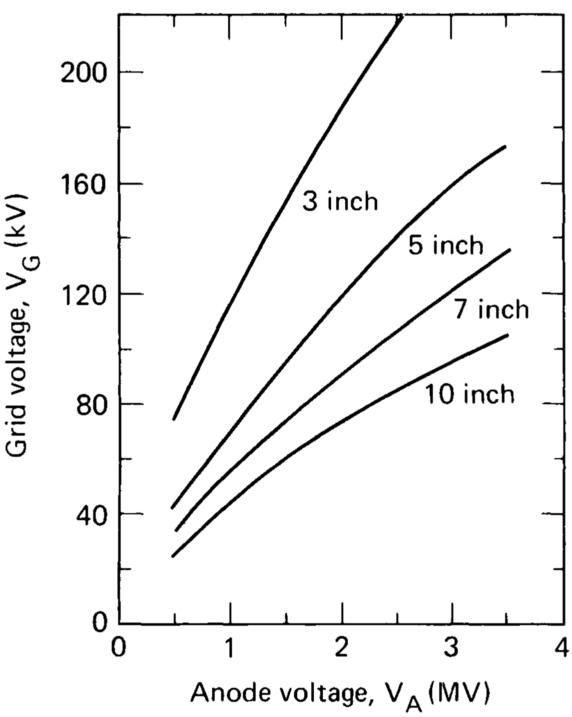

FIGURE 8 Limiting grid voltage for virtual cathode formation vs anode voltage for 4 cathode diameters.

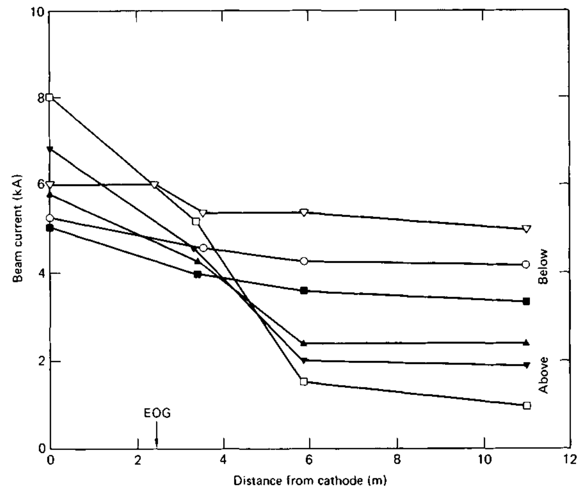

FIGURE 9 Peak beam current measured at the cathode and several positions in the accelerator for the experiments represented in Fig. 7.

transported to the end of the accelerator is high. These results are shown in Figs. 7 and 9. Figure 7 shows values of cathode current vs V_a for eight experiments. Three data points represent cathode current above the computationally determined limiting current, and five data points represent cathode current below this limiting current. Figure 9 shows the peak beam current measured at the cathode and various positions along the entire accelerator for the experimental parameters shown in Fig. 7. When the cathode current lies above the limiting current in Fig. 7, only one-fourth to one-third of the current extracted from the cathode reaches the current monitor 6 m from the cathode. When the cathode current lies below the limiting current in Fig. 7, at least three-fourths of the cathode current reaches the end of the machine.

A possible explanation of these results is that indeed a virtual cathode does form downstream from the grid, but the virtual cathode can act as a source of electrons. No calculations can be performed with the EBQ code in the regime of virtual cathode formation, but it is known that plasma oscillations occur in a virtual cathode. Particles can be emitted with large random velocities so that any beam accelerated from a virtual cathode would have poor quality (i.e., the emittance is high) and be impossible to transport efficiently. The virtual cathode forms in a small region near the axis, but the time-dependent electric field generated in this region extends over the entire beam cross-section, distorting the trajectories of particles outside the region. Thus the emittance of the entire beam is increased to the point that only a small fraction of the particles emitted from the cathode are transported to the end of the accelerator.

REFERENCES

1. A. C. Paul and V. K. Neil, Computational Studies of Beam Dynamics in the ETA Gun, *IEEE Trans. Nucl. Sci. NS-26*, 4242 (1979).
2. J. E. Bohs and D. Kelleher, *J. App. Phys. 40*, 6 (1969). See also H. R. Jory and A. W. Trivelpiece, *J. App. Phys. 40* 10 (1969).